

Article

Electron Probe Micro-Analyzer Studies and Raman Spectroscopic Characterization of Plagioclase in Basaltic Rocks from the Asal–Ghoubbet Area, Republic of Djibouti

Awaleh Djama Iltireh ^{1,*}  and Yusuf Kağan Kadioğlu ^{2,3}¹ Graduate School of Natural and Applied Sciences, Ankara University, Ankara 06110, Turkey² Department of Geological Engineering, Ankara University, Ankara 06830, Turkey; kadi@ankara.edu.tr³ Earth Sciences Application and Research Center (YEBİM), Ankara University, Ankara 06830, Turkey

* Correspondence: awalehiltireh@gmail.com

Abstract: The Asal–Ghoubbet Rift area comprises basaltic rocks with similar compositions that were formed by volcanic eruptions. To gain insight into the magmatic processes of these volcanic formations, we investigated the mineral chemistry of plagioclase macrocrysts and microcrysts found in the basaltic rocks by using an electron probe micro-analyzer (EPMA). These basaltic rocks contain olivine, pyroxene, euhedral plagioclase macrocrysts, and euhedral to subhedral plagioclase microcrysts. These plagioclase macrocrysts reach up to 4 cm in length in the form of giant crystals as plagioclase ultraphyric basalts (PUBs). They have a mineral composition varying from bytownite to labradorite with anorthite content ranging from An₅₃ to An₈₆. Also, the microcrysts of all these volcanic rocks are characterized by labradorite and andesine compositions with An_{22–80}. According to the calculated plagioclase thermobarometry, the crystallization temperature of the plagioclase macrocrysts and microcrysts is 1082 to 1216 °C and 1072 to 1203 °C, respectively, and the pressure is 3.92 to 14.51 kbar for the macrocrysts and 2.99 to 14.84 kbar for the microcrysts. Based on these thermobarometry results for the plagioclases, we conclude that the volcanic formations located in the Asal–Ghoubbet area would have come from different eruptions from a single magmatic chamber.



Citation: Iltireh, A.D.; Kadioğlu, Y.K. Electron Probe Micro-Analyzer Studies and Raman Spectroscopic Characterization of Plagioclase in Basaltic Rocks from the Asal–Ghoubbet Area, Republic of Djibouti. *Minerals* **2024**, *14*, 216. <https://doi.org/10.3390/min14030216>

Academic Editor: Zhaochong Zhang

Received: 23 January 2024

Revised: 11 February 2024

Accepted: 15 February 2024

Published: 21 February 2024

Keywords: Asal–Ghoubbet; EPMA; mineral chemistry; PUB; thermobarometry; magma chamber

1. Introduction

This study was carried out in the Asal–Ghoubbet area, located in the Republic of Djibouti, which is characterized by volcanoes, fissures, basaltic rocks, and fumaroles. It is an area in which major extensional tectonic, magmatic, and seismic activity takes place [1]. The Asal Rift is considered to be a recently emerged section of the Tadjourah Ridge with a change in tectonic direction from the NE–SW direction characterizing the Tadjourah axis to NW–SE in the Asal Rift [1]. This rift is 12–15 km long and 3–6 km wide, and it is bordered by Lake Asal to the northwest and Ghoubbet Shark Bay to the southeast [1–3]. The Asal Rift is made up of successive steps lowered relative to each other by normal faults [2,4].

The entire Asal Rift graben is covered with recent to subcurrent basaltic traps [1]. The basalt of the Asal Rift lava flows corresponds to highly vesiculated basalts characterized by an aphyric texture and porphyritic basalts with a plagioclase, olivine, and clinopyroxene mineral assemblage [5]. These basaltic traps are characterized by an extreme abundance of large plagioclase phenocrysts whose size can reach several centimeters and that are always associated with numerous gas bubbles [1]. The basalt rocks that outcrop in the Asal–Ghoubbet area come from volcanoes such as Fialé, Galaé’le Koma, and Inki Garayto and eruptive fissures such as the Manda and Ardoukoba volcanoes, as well as the marginal basalts [6]. The lavas of the Asal–Ghoubbet area are characterized by pahoehoe and aa, and the latter is the most common lava type in the rift region [6,7].



Copyright: © 2024 by the authors. Licensee MDPI, Basel, Switzerland. This article is an open access article distributed under the terms and conditions of the Creative Commons Attribution (CC BY) license (<https://creativecommons.org/licenses/by/4.0/>).

Plagioclase can be used as a key in the determination of the position of supplementary basaltic magma. The plagioclase ultraphyric basalt (PUB) is used in the explanation of the source of the host magma. The accumulation of the macrocrysts of the plagioclase within the basalt may be indicative of slow rift spreading and the keeping of the high temperature for the crystallization of macrocrysts of the plagioclases [8–10].

The goal of this research is to determine the compositional differences of the giant and micro crystals of the plagioclases and their genesis by using Raman spectral spectrometry and EPMA mineral chemistry. The analyzed rock samples representing these volcanic rocks contain olivine, pyroxene, and plagioclase. Characterizing the mineral chemistry of plagioclase would provide a helpful understanding of the physical, chemical, and thermodynamic conditions through which the mineral was formed and may also provide beneficial data for the assessment of crystallization history and the nature of the magma. In this work, we focus on the plagioclase mineral chemistry of the different volcanic rocks.

2. Geological Background

In the Republic of Djibouti, the extensional plate boundary between the African and Arabian plates, trends east–west along the Gulf of Aden and Gulf of Tadjourah axis and penetrates inland toward the volcanic ranges of the Afar Depression [4,11,12]. The Asal Rift is the first emergent segment of the Aden Ridge, which propagates westward on land into the Afar Depression [12,13]. The Asal–Ghoubbet area covers a narrow area, approximately 12 to 15 km wide [3].

The Asal Rift represents an active tectonic–volcanic axis of basaltic nature built on a system of northwest faults and fissures that is similar to the other axial chains in the Afar (Figure 1). It is associated with active volcanism, significant seismicity, and an abnormally high geothermal flux [4,11]. These volcanic ranges are currently thought to be the exposed structures equivalent to mid-oceanic ridge valleys [14]. The Asal–Ghoubbet Rift forms the oldest of these areas and the transition between submarine and subaerial segments of the ridge, and the rift has been considered an active spreading center with features similar to those of axial oceanic rift valleys [1,11,15,16].

This zone is affected by NE–SW dismantling tectonism, which divides it into parallel NW–SE panels whose relative collapse has individualized margins and an internal floor where tectonic and magmatic activity is currently manifested [3]. In the Asal–Ghoubbet Rift, continental deformation has created normal faults oriented NW–SE, which leads to an extension of the blocks. This NW–SE tectonic pattern predominates and is the main orientation. Recent normal faults and open fissures align parallel to this tectonic direction, which is therefore the current orientation of the rift [1].

The Asal Rift opened during the Pleistocene within a tectonized basaltic and rhyolitic stratoid series of Mio–Pliocene age, and these series are found commonly along the margins of the Afar Depression [4]. Massive hyaloclastites generally marked the beginning of the rifting and the first rise of magma through the cracks thus formed [1]. Opened after the Pliocene, the hyaloclastites are superimposed unconformably on a series of predominantly alkaline basalts. The rift produced lavas of tholeiitic affinity, poor in potassium, comparable to those of neighboring oceanic ridges. These lavas range from magnesian basalts to ferro-basalts with MgO 3.00–8.00 and K₂O 0.10–0.90. The geographical distribution of the different petrographic terms is not random; the most evolved lavas are grouped in the axial valley [4]. The age of the volcanic rocks located in the Asal–Ghoubbet area is less than 0.7 Ma [2,17].

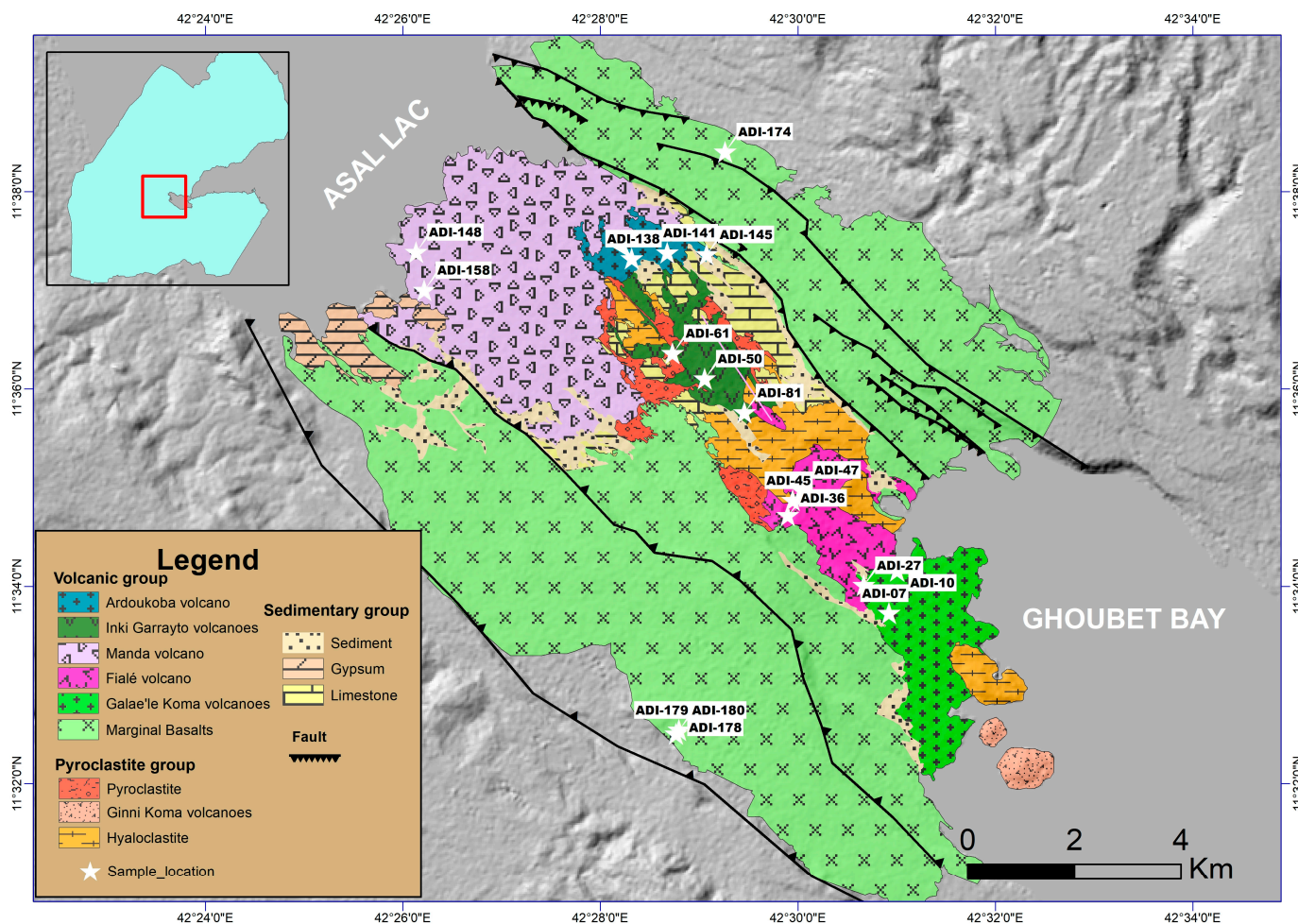


Figure 1. Geological map of the Asal–Ghoubbet Rift simplified from [18] combined with the SRTM DEM, showing the different volcanic formations. In the top left, the Republic of Djibouti shapefile map and a square representing the study area.

Based on its size and the shape of the median valley, as well as a certain number of tectonic features and the composition of certain lavas, the Asal Rift is comparable to oceanic ridges. The youngest lavas and tectonic structures of the rift are located within the axial valley. These lavas differ from those in the rift margins by the nature of the primary magma and its degree of fractionation. There is a petrographic evolution of products emitted from the margins toward the axial valley; lavas within the margins are predominantly porphyritic, contrasting with the generally aphyric textures that occur in the axial valley lavas [4]. The isotopic $^{206}\text{Pb}/^{204}\text{Pb}$ ratios of Asal basalts correspond to half of the planet-wide oceanic field (MORB and OIB) [19]. Also, the isotopic data on Asal basalts fall in the part of the mixing hyperbola between P-type and N-type MORBs [20].

In this region, the lavas exposed in the Asal–Ghoubbet area comprise the marginal basalts, Galae'le Koma, Fialé, Manda, Inki Garayto, and Ardoukoba (Figure 2). These volcanic formations of Asal constitute a series of basaltic lavas with variable but continuous compositions ranging from magnesian to iron-rich. The lavas rich in plagioclase phenocrysts may belong to several of these basaltic formations, and these lavas were produced by the accumulation of crystals in a magma whose chemical and mineralogical composition had evolved [1]. Furthermore, petrological and geochemical data suggest that the origin of all the Asal rocks cannot be simply attributed to the fractionation of a single primary magma; the variation observed in the different basaltic terms could be considered to be linked to changes in the rate of melting within the mantle [4].



Figure 2. Field pictures of the Asal–Ghoubbet area, showing where the investigated volcanic units are exposed: (a) marginal basalts, (b) Galaé’le Koma, (c) Fialé, (d) Manda, (e) axial volcanic chains of Inki Garayto, and (f) Ardoukoba.

Most Asal Rift lava flows are highly vesiculated basalts. The aphyric texture is present in 64% of the basalts sampled along the margins of the rift. Most of the lava flows of the

inner floor (75%) correspond to porphyritic basalts with plagioclase megacrysts (8% to 54%), and olivine (0.1% to 6%) and clinopyroxene (5%) in smaller proportions. The bulk of these mineral phases have a similar chemical composition with different proportions. The plagioclase megacrysts correspond to bytownite of An_{76-88} with a size that can reach 1 cm, which is unusual in eruptive rocks. Some plagioclase crystals are subhedral, and most display melt inclusions, anhedral outlines, or corroded boundaries [5]. The bytownite megacrysts are almost all perfectly euhedral and have a relatively homogeneous composition with limited variation in their anorthite contents (from $An_{81.5}$ to An_{88}) except for their extreme edge, which is approximately An_{70} [7].

3. Sampling and Analytical Methods

In total, 148 rock samples were collected from the marginal basalts (22 samples), Galaé'le Koma volcanoes (34 samples), Fialé volcano (22 samples), Manda volcano (22 samples), Inki Garayto volcanoes (23 samples), and Ardoukoba volcano (25 samples). Sampling sites are shown on the geological map (Figure 1). For all of these rock samples, thin sections were prepared in the thin section laboratory at Ankara University Earth Sciences Application and Research Center (YEBİM) and observed using a Zen polarizing microscope in the Center's petrography research laboratory.

To determine the types of plagioclase minerals, confocal Raman spectroscopy (CRS) studies were performed using equipment from YEBİM [21–23]. For this study, the Raman spectrometry investigations involved different point analyses of six samples representing the different volcanic units of the well-characterized plagioclase minerals. These samples were selected according to the main lithological differentiation in the field and petrographic studies. The selected samples represent all the subunits of the volcanic eruptions in the Asal–Ghoubbet area.

After an initial petrographic investigation, 18 thin sections were selected for plagioclase chemistry analysis by using an electron microprobe. These selections were based on euhedral plagioclase from each thin section prepared for this study. The total number of plagioclase crystal points analyzed was 533; the results together with the whole-rock data are reported in Tables S1–S7 in the Supplementary Materials section. Acquisitions were carried out using a JEOL JXA-8230 instrument located at YEBİM EPMA Laboratory, which is equipped with five wavelength-dispersive spectrometers. The operating conditions were 20 kV accelerating voltage and 20 nA beam current. Natural oxide and mineral reference materials were used for calibration and measurements following the methods described in [24].

4. Results

Detailed petrography, whole-rock major element geochemical data, trace element geochemical data, and isotope geochemistry of the volcanic units are presented in [6].

4.1. Petrography and Mineral Chemistry

The marginal basalt comprises porphyritic and aphyric basalts. In porphyritic rocks, the size of plagioclase macrocrysts is greater than 2 cm. The texture of these rocks varies from euhedral to subhedral texture (Figure 3a). The large plagioclase phenocryst suggests their formation under equilibrium conditions, and some show polysynthetic twinning. In aphyric rocks, plagioclase macrocrysts have a subhedral texture and dimensions of 1 mm or less. All plagioclase minerals were observed to have a glomeroporphyritic texture. In some samples, the plagioclases show an embayment texture due to the resorption of olivine, other plagioclases, and matrix. Plagioclases mostly contain opaque minerals, and rarely plagioclase, pyroxene, and olivine inclusions, and exhibit a poikilitic texture. The mineral chemistry of these plagioclases generally spreads from bytownite to andesine (Figure 4a). The anorthite content of the macrocrysts varies between An_{59} and An_{84} , and they have a composition varying from bytownite to labradorite. These macrocrysts generally show oscillatory zoning. The plagioclase microcrysts show An_{43-74} and have oscillatory and

normal zoning. These microcrysts show that the composition varies from labradorite to andesine.

The Galaé'le Koma volcanoes are characterized by porphyritic and vesicular basalts. The plagioclases in these basalts are observed as giant crystals and microcrysts within the matrix. The dimensions of plagioclase macrocrysts are greater than 2 cm. Their textural features vary from euhedral to subhedral in all the determined thin sections. The features shown in all of the plagioclases suggest crystallization in a condition of equilibrium and exhibit normal zoning. They show both Carlsbad and polysynthetic twinning in some samples and only polysynthetic twinning in other samples (Figure 3b). All plagioclases were crystallized side by side into a glomeroporphyritic texture. In some plagioclase macrocrysts, a deep embayment texture is observed, and occasionally this embayment is filled by the matrix. Plagioclases contain inclusions of olivine crystals and opaque minerals with a poikilitic texture. Plagioclases exhibiting a sieve texture are rarely seen. The plagioclase minerals exhibit different compositions ranging from labradorite to bytownite and andesine (Figure 4b). Macrocryst minerals have a composition of An_{79-83} and exhibit oscillatory and normal zoning. These phenocryst minerals are richer in anorthite content and are more calcic. Plagioclase microcrysts have An_{36-59} and exhibit normal zoning. The composition of these microcrysts varies from labradorite to andesine.

The plagioclases of Fialé basalt are characterized by giant macrocrysts, microcrysts, and microliths formed in the matrix. The size of macrocrysts can reach up to 3–4 cm. Macrocrysts have a generally euhedral to subhedral texture. The plagioclases contain abundant plagioclase microcrysts, plagioclase microlites, and opaque mineral inclusions. They also contain olivine and clinopyroxene inclusions exhibiting a poikilitic texture (Figure 3c). The plagioclase minerals exhibit a glomeroporphyritic texture. Polysynthetic twinning was observed in all plagioclase macrocrysts. Plagioclase macrocrysts of Fialé volcano exhibit bytownite composition and smaller labradorite composition. Their anorthite content varies between An_{61} and An_{86} , and they show oscillatory zoning. Plagioclase microcrysts have andesine and, rarely, oligoclase compositions. These plagioclase microcrysts have a composition of An_{22-49} and show normal zoning (Figure 4c).

The plagioclase mineral of Manda volcano occurs as macrocrysts and microcrysts. Macrocrysts have large dimensions, up to 2 cm. They are characterized by euhedral and subhedral textures. They exhibit both Carlsbad and polysynthetic twinning in some basaltic samples and macrocrysts without twinning in the same samples (Figure 3d). All plagioclases have a glomeroporphyritic texture. Some plagioclases have been absorbed by the other plagioclases, exhibiting an embayment texture. Plagioclases mostly contain opaque minerals and olivine microcrysts as inclusions. The plagioclase macrocrysts of Manda volcano have a bytownite composition with An_{74-83} . These macrocrysts show oscillatory and normal zoning. Plagioclase microcrysts exhibit labradorite and andesine compositions. Plagioclases have An_{35-69} content and exhibit reverse zoning and normal zoning (Figure 4d).

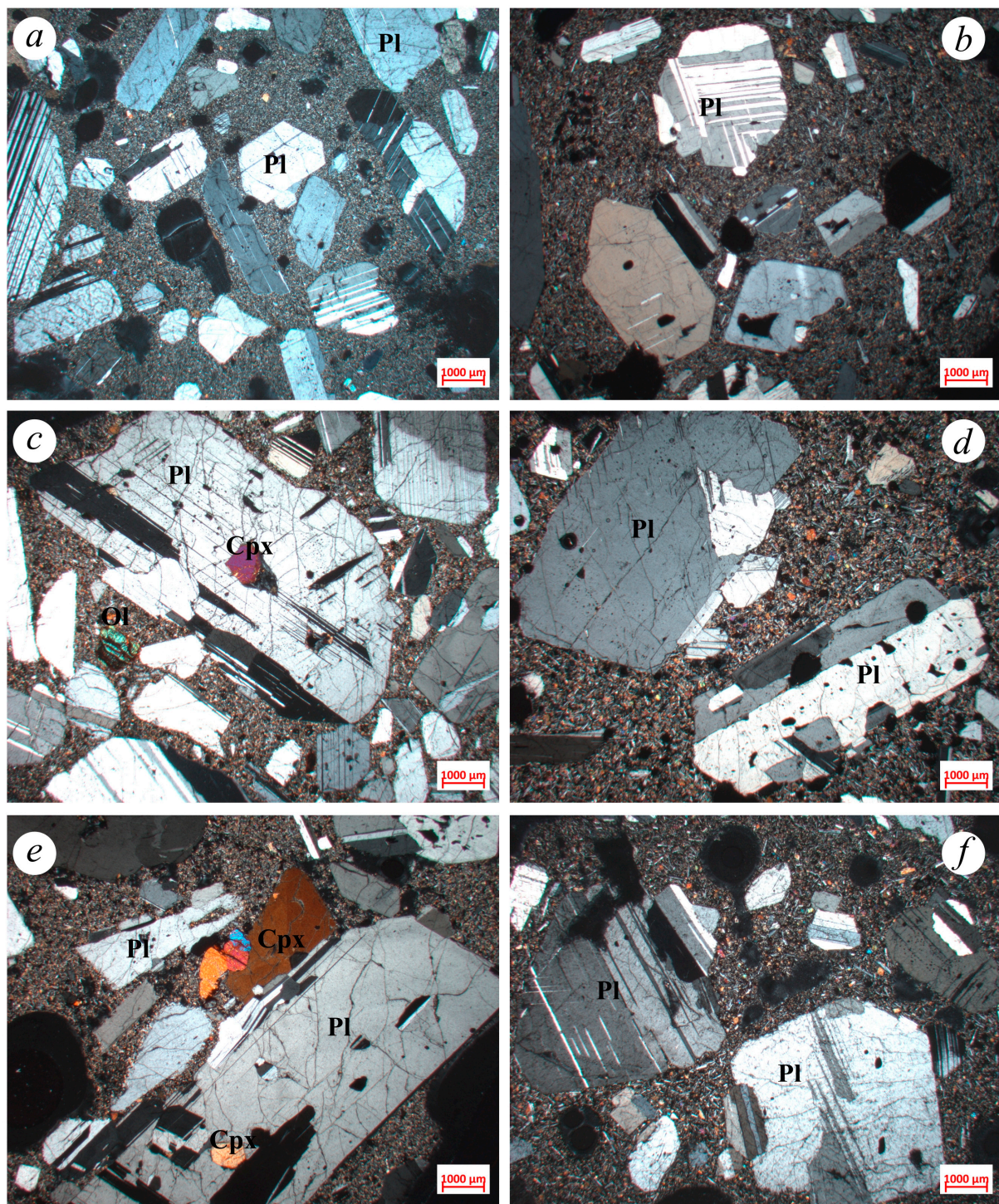


Figure 3. Representative microphotographs of basaltic rocks from the Asal-Ghoubbet area: (a) marginal basalts, (b) Galaé'le Koma, (c) Fialé, (d) Manda, (e) Inki Garayto, (f) Ardoukoba.

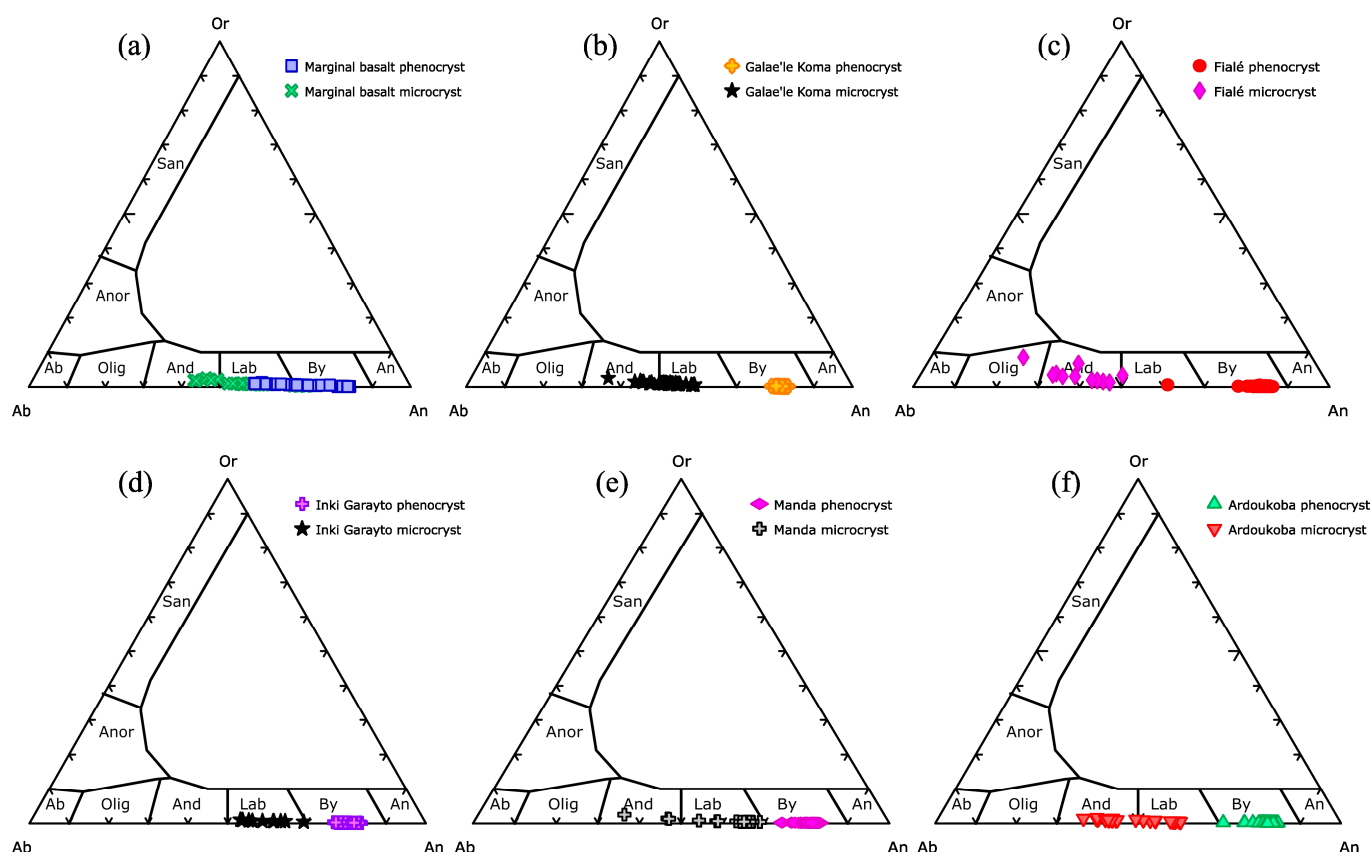


Figure 4. Composition of plagioclase in the volcanic rocks from the Asal–Ghoubbet area: (a) marginal basalts, (b) Galae’le Koma, (c) Fialé, (d) Inki Garayto, (e) Manda, and (f) Ardoukoba.

The volcano of Inki Garayto and the associated parasitic volcanoes form an axial chain oriented NW–SE and lie perpendicular to the opening axis of the Asal–Ghoubbet Rift. The lava extruded by these various volcanic cones has an aa-type character. These lavas that erupted in different eruption centres can be divided into two groups: porphyritic basalt and basaltic trachy-andesite [6,25]. The plagioclase in the porphyritic basalt from Inki Garayto occurs as macrocrysts and microcrysts. The macrocrysts have a 4 cm size and have euhedral to subhedral texture. The plagioclase phenocrysts are clustered into a glomeroporphyritic texture. We observed in the same samples that the plagioclases have Carlsbad and polysynthetic twins, and there is also a plagioclase without twins. The inclusion of plagioclase, olivine, pyroxene, and opaque minerals as a poikilitic texture is seen in the plagioclase macrocrysts (Figure 3e). The macrocrysts of plagioclases are corroded and embayed deeply by an intergranular texture matrix and by some macrocrysts of plagioclase and clinopyroxene minerals. In the petrographic examination of Inki Garayto volcanoes, basalt and basaltic trachy-andesite rocks are revealed. These plagioclase macrocrysts show a composition of An_{53-69} . They show oscillatory zoning. The plagioclase microcrysts of these basaltic rocks have a composition that varies between An_{67} and An_{80} (Figure 4e). These microcrysts have oscillatory zoning.

The basaltic trachy-andesite lavas of the Inki Garayto volcanoes have a mineralogical assemblage of plagioclase and clinopyroxene and an opaque mineral composition. The rocks are dominated by the component matrix of plagioclase microlite in trachytic texture. Plagioclase occurs in microcrysts and microlites 1–2 mm in size and with a euhedral to subhedral texture [25].

The plagioclase minerals of Ardoukoba volcano occur as macrocrysts and microcrysts in the groundmass. The macrocrysts range in size up to 2 cm. Their textures vary from euhedral to subhedral, and other samples show a subhedral to anhedral texture. All the

plagioclase minerals crystallized under a condition of equilibrium and show twinning. They exhibit both Carlsbad and polysynthetic twinning in some samples and only polysynthetic twinning in the major samples. There are also some samples that present plagioclases with twinning and without twinning (Figure 3f). Zoning is also present in some samples. We observed that all plagioclases have a glomeroporphyritic texture. Some plagioclases have undergone an embayment of microlithic groundmass and, occasionally, plagioclase crystals and olivine microcrysts. The plagioclases enclosed small opaque minerals and olivine as inclusions. Some of the plagioclase macrocrysts also have pyroxene inclusions in rare amounts. Plagioclase macrocrysts have a composition of An_{71-84} (Figure 4f). These plagioclases show oscillatory zoning. The microcrysts exhibit labradorite and andesine compositions. They have a composition of An_{39-60} and show oscillating and normal zoning.

4.2. Raman Characteristics of Plagioclases

The petrographic examinations reveal that the plagioclase macrocrysts are bytownite. In contrast, the confocal Raman spectrometry (CRS) method reveals that in the marginal basalts, Manda, and Ardoukoba rocks, plagioclases are bytownite, while rocks in the Inki Garayto volcanoes have anorthite compositions. Plagioclases from Galaé'le Koma and Fialé volcanoes exhibit anorthite to labradorite and bytownite to anorthite compositions, respectively (Figures S1 and S2).

As a result of the confocal Raman spectrometry (CRS) study carried out on the plagioclase minerals in the rocks in the marginal basalts, it was determined that the plagioclases had a bytownite composition. The following Raman spectra of this bytownite composition were observed: 984.42, 748.53, 693.43, 559.70, 508.31, 490.36, 430.92, and 285.43 cm^{-1} (Figure S1).

The composition of the plagioclase minerals in the rocks representing Galaé'le Koma volcanoes is generally labradorite and anorthite. It has Raman shifts at 1117.43, 741.50, 570.45, 514.46, 485.54, 408.01, and 203.74 cm^{-1} , which indicate a labradorite composition. The anorthite composition exhibits Raman shifts at 734.73, 566.14, 513.23, 489.23, 410.48, 284.96, and 190.82 cm^{-1} (Figure S2).

Plagioclase minerals with a bytownite composition in Fialé volcano have strong Raman shifts at 733.68, 510.17, 490.36, 681.67, 511.41, and 168.37 cm^{-1} . In addition to these peaks, weak shifts are also observed at 981.95, 276.76, and 280.47 cm^{-1} (Figure S2). Plagioclase with an anorthite composition has Raman shifts at 749.77, 507.69, 742.34, and 507.17 cm^{-1} (Figure S2).

Basaltic rocks of Manda volcano were found by confocal Raman spectrometry studies to have a composition of the plagioclase mineral bytownite. Raman shifts are observed for plagioclase mineral with a bytownite composition at 1117.33, 1115.06, 824.09, 739.25, 642.36, 564.65, 564.12, 512.03, 488.96, 486.64, 407.02, 395.63, 286.89, 276.14, 204.34, and 189.46 cm^{-1} (Figure S1).

A confocal Raman spectrometry (CRS) study carried out on the basalts of the Inki Garayto volcanoes reveals the anorthite composition of plagioclase minerals. This anorthite mineral has a strong Raman shift at 741.13 and 508.99 cm^{-1} , and in addition to these peaks, weak shifts are also observed at 1118.82, 565.49, and 404.59 cm^{-1} (Figure S2).

Based on the Raman spectral shift characteristic, the plagioclase from Ardoukoba volcano has a bytownite composition. Bytownite has strong Raman shifts at 508.67, 488.96, 512.03, 739.25, and 486.64 cm^{-1} , and in addition to these peaks, weak shifts are also observed at 395.63, 276.14, and 286.89 cm^{-1} (Figure S1).

According to the results obtained from Raman spectrometry, the macrocrysts of all these volcanoes have anorthite and bytownite compositions, and the microcrysts have labradorite compositions.

4.3. Major Element Composition of Plagioclases

Representative plagioclase macrocrysts and microcrysts were selected for rim-to-core transects using electron probe microprobe analysis. Major element compositions of the

marginal basalts, Galaé'le Koma volcanoes, Fialé volcano, Manda volcano, Inki Garayto volcanoes, and Ardoukoba volcano are reported in Supplementary Tables S2–S7.

The plagioclase macrocrysts and microcrysts have concentrations of SiO_2 (49.45–57.41 wt.%), Al_2O_3 (28.47–34.92 wt.%), and CaO (6.67–15.30 wt.%), moderate Na_2O content (1.63–4.99 wt.%), and low concentrations of FeO_T , MgO , K_2O , and TiO_2 .

Concerning the samples from the Galaé'le Koma volcanoes, the geochemical variations in plagioclase macrocrysts and microcrysts show a wide range in mineral chemistry. The plagioclase macrocrysts exhibit a content of SiO_2 ranging from 48.23 to 51.04 wt.%; Al_2O_3 from 31.32 to 34.25 wt.%; CaO from 14.13 to 14.98 wt.%; Na_2O from 1.65 to 2.10 wt.%; $\text{FeO}_T > 1$ wt.%; and low content of TiO_2 , MgO , and K_2O . The plagioclase microcrysts are characterized by SiO_2 content ranging from 52.29 to 58.42 wt.%; Al_2O_3 from 26.86 to 29.28 wt.%; CaO from 7.22 to 11.76 wt.%; Na_2O from 4.48 to 6.96 wt.%; FeO_T from 0.76 to 2.83 wt.%; and low content of TiO_2 , MgO , and K_2O .

In Fialé volcano, the mineral chemistry concentrations of plagioclase macrocrysts and microcrysts exhibit considerable variability that is related to slow cooling during macrocryst crystallization and rapid cooling during microcryst crystallization. The macrocrysts of Fialé volcano exhibit a SiO_2 content of 45.46–49.80 wt.%, Al_2O_3 content of 30.16–35.02 wt.%, CaO content of 12.43–16.68 wt.%, Na_2O content of 1.42–4.36 wt.%, and FeO_T less than 1 wt.%, while the plagioclase microcrysts show a SiO_2 content of 54.81–59.65 wt.%, Al_2O_3 content of 20.58–28.28 wt.%, and Na_2O content of 5.41–7.71 wt.%, along with CaO (4.47–9.90 wt.%) and a low concentration of FeO_T (0.77–3.88 wt.%).

Regarding the chemical composition of Manda volcano, the SiO_2 , Al_2O_3 , CaO , and Na_2O contents of plagioclase macrocrysts were 47.95–51.71 wt.%, 30.15–33.52 wt.%, 14.43–16.00 wt.%, and 1.77–2.76 wt.%, respectively, with a concentration of less than 1 wt.% for FeO_T , MgO , and TiO_2 . The plagioclase microcrysts have SiO_2 , Al_2O_3 , CaO , Na_2O , and FeO_T concentrations that range from 51.10 to 55.57 wt.%, 23.30 to 30.92 wt.%, 7.53 to 13.34 wt.%, 3.53 to 7.39 wt.%, and 0.48 to 1.24 wt.%, respectively, and also low concentrations of MgO and TiO_2 .

The Inki Garayto samples have a plagioclase macrocryst composition of SiO_2 ranging from 48.74 to 52.99 wt.%, Al_2O_3 from 28.98 to 34.19 wt.%, CaO from 14.08 to 15.31 wt.%, and Na_2O from 1.62 to 2.37 wt.% and a very low content, less than 1 wt.%, of FeO_T , MgO , K_2O , and TiO_2 . The plagioclase microcrysts show SiO_2 content ranging from 48.74 to 55.98 wt.%, Al_2O_3 from 26.42 to 34.19 wt.%, CaO from 10.29 to 15.31 wt.%, and Na_2O from 1.62 to 4.99 wt.% and very low content, less than 1 wt.%, of FeO_T , MgO , K_2O , and TiO_2 .

The Ardoukoba volcano samples displayed a narrow range in plagioclase macrocryst composition, with SiO_2 content ranging from 46.13 to 50.00 wt.%; Al_2O_3 content from 31.09 to 34.77 wt.%; a narrow range in CaO content from 14.03 to 16.32 wt.%; Na_2O content from 1.61 to 5.99 wt.%; and low concentrations, less than 1 wt.%, of FeO_T , MgO , K_2O , and TiO_2 . The plagioclase microcrysts display a wide range in SiO_2 from 52.00 to 59.00 wt.%, narrow content of Al_2O_3 from 25.37 to 29.99 wt.%, CaO content from 6.18 to 12.03 wt.%, and high content of Na_2O ranging from 4.33 to 5.99 wt.%. The FeO_T , MgO , K_2O , and TiO_2 concentrations are less than 2 wt.%.

The volcanoes located in the Asal–Ghoubbet area, which are the Ardoukoba volcano, Inki Garayto volcanoes, Manda volcano, Fialé volcano, the Galaé'le Koma volcanoes, and the marginal basalts, can be classified into one group based on their respective plagioclase composition characteristics. The plagioclases have a similar major element composition for SiO_2 , Al_2O_3 , CaO , Na_2O , FeO_T , MgO , K_2O , and TiO_2 and exhibit little variation (Figures 5 and 6).

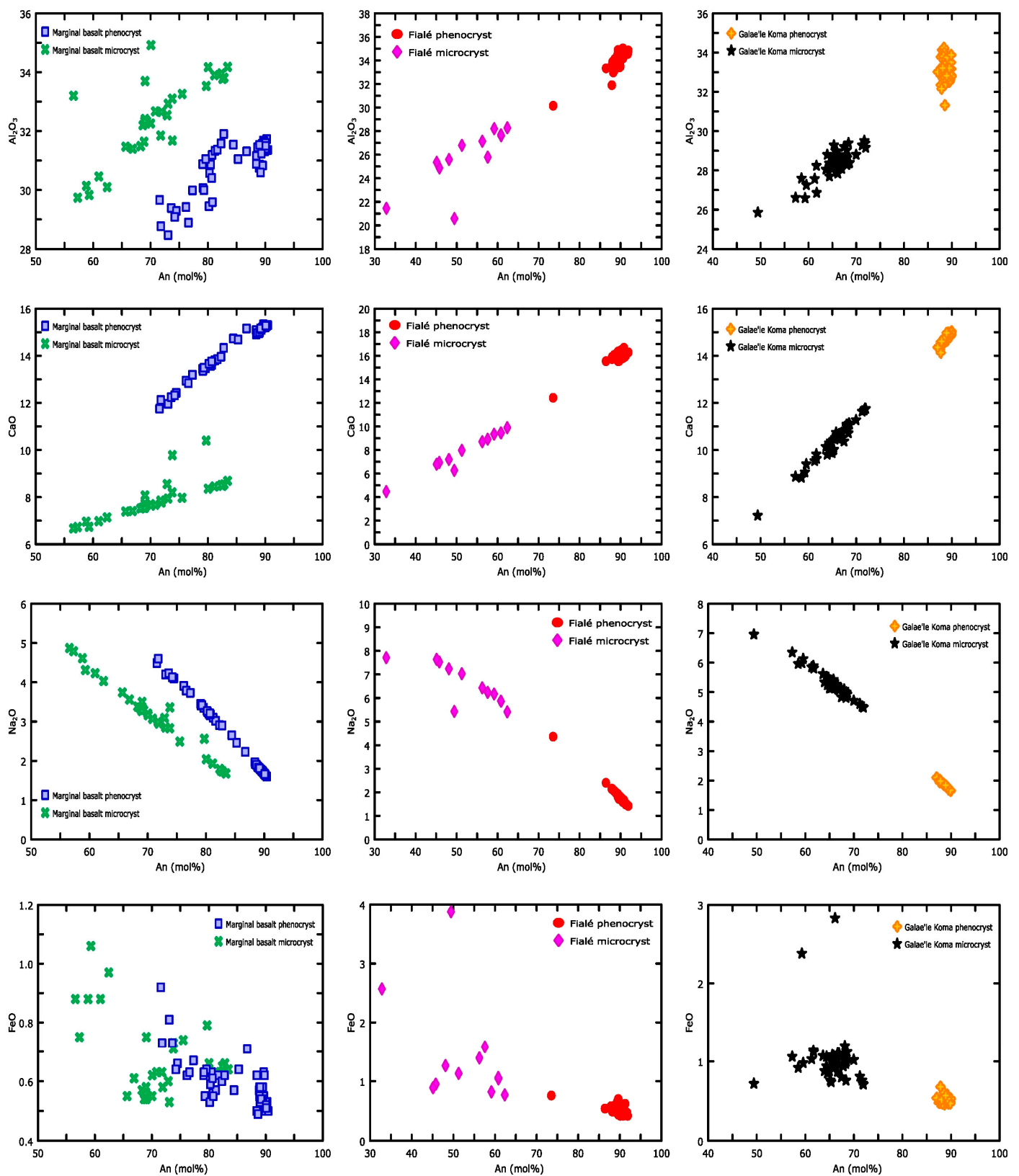


Figure 5. Major element variation diagram showing Al_2O_3 , CaO, Na_2O , and FeO_T versus An (mol%) from the marginal basalts, Fialé volcano, and Galaé'le Koma volcanoes.

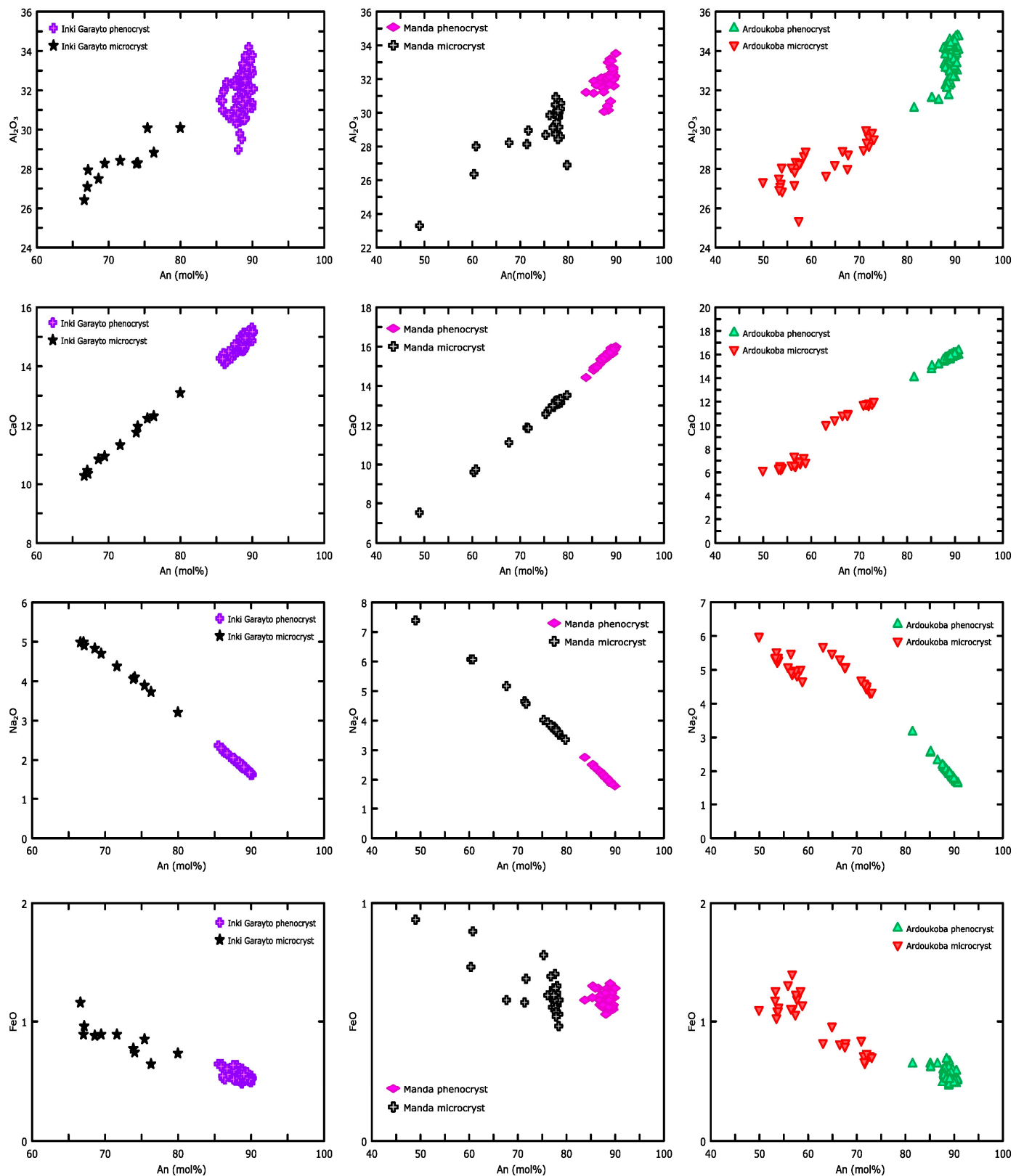


Figure 6. Major element variation diagram showing Al₂O₃, CaO, Na₂O, and FeO_T versus An (mol%) from Inki Garayto volcanoes, Manda volcano, and Ardoukoba volcano.

5. Discussion

5.1. The Nature of Plagioclases

The major element geochemistry of the plagioclase macrocrysts and microcrysts of all basaltic rocks from the Asal–Ghoubbet area was plotted together to observe their relationship and magma source variation (Figure 7). The rapid cooling of the magma may act to lower differentiation during the magma crystallization, increasing the amount of the microcryst of the plagioclases. The diagrams showing the variation in Al_2O_3 and CaO versus SiO_2 for these volcano products show that the plagioclase macrocrysts and microcrysts have high Al_2O_3 content and CaO content, which is typical for a mantle source product. The low amount of FeO_T and MgO reflects a decrease in the amount of pyroxene and olivine in the whole-rock compositions. The Na_2O content of these plagioclases is low to moderate, meaning they are also mantle source products. These results correspond with those reported by [26], which indicate that the MgO content of the parent melt for the plagioclase macrocrysts is calculated to be <0.5 wt.% and that FeO_T ranges from 0.5 to 1.1 wt.%. Similarly, all these basaltic rocks have strong similarities and are genetically related. This suggests that the source of these different volcanic formations located in the Asal–Ghoubbet area is a single magmatic reservoir. Also, the interpretation of these data can lead to understanding the behaviour of the magma chamber that produced different eruptions during the period of volcanic activity. This magma chamber might be the main source of these eruptions, taking the form of a unique magma source, like a mantle plume.

Moreover, ref. [27] suggests that the petrographic diversity and geochemical variation in the lavas from the Asal–Ghoubbet area are largely due to the strong fractional crystallization of the magmas. This fractional crystallization can occur throughout the ascent of magmas from upper mantle zones, and the geochemical study of samples belonging to lavas from the recent axial series provides proof of the essential role of fractional crystallization [27].

5.2. H_2O Content

While the status of the plagioclase–melt barometer is certainly questionable, the plagioclase–melt equilibrium can be useful as a hygrometer, at least if the temperature (T °C) is well known [28]. For this, we used the model proposed by [28] to calculate the plagioclase–liquid hygrometer to constrain the pre-eruptive melt H_2O contents in all volcanic rocks from the Asal–Ghoubbet area. The method is based on the crystal–liquid exchange reaction between the albite and anorthite components. Calculated H_2O contents in samples from Ardoukoba volcano range from 0.58 to 4.16 wt.%, Inki Garayto volcanoes from 2.39 to 4.15 wt.%, Manda volcano from 1.74 to 3.83 wt.%, Fialé volcano from 1.11 to 4.42 wt.%, Galaé’le Koma volcanoes from 0.24 to 3.90 wt.%, and the marginal basalts from 0.23 to 4.19 wt.%. The H_2O content of the macrocrysts and microcryst samples from these volcanoes is summarized below (Table 1).

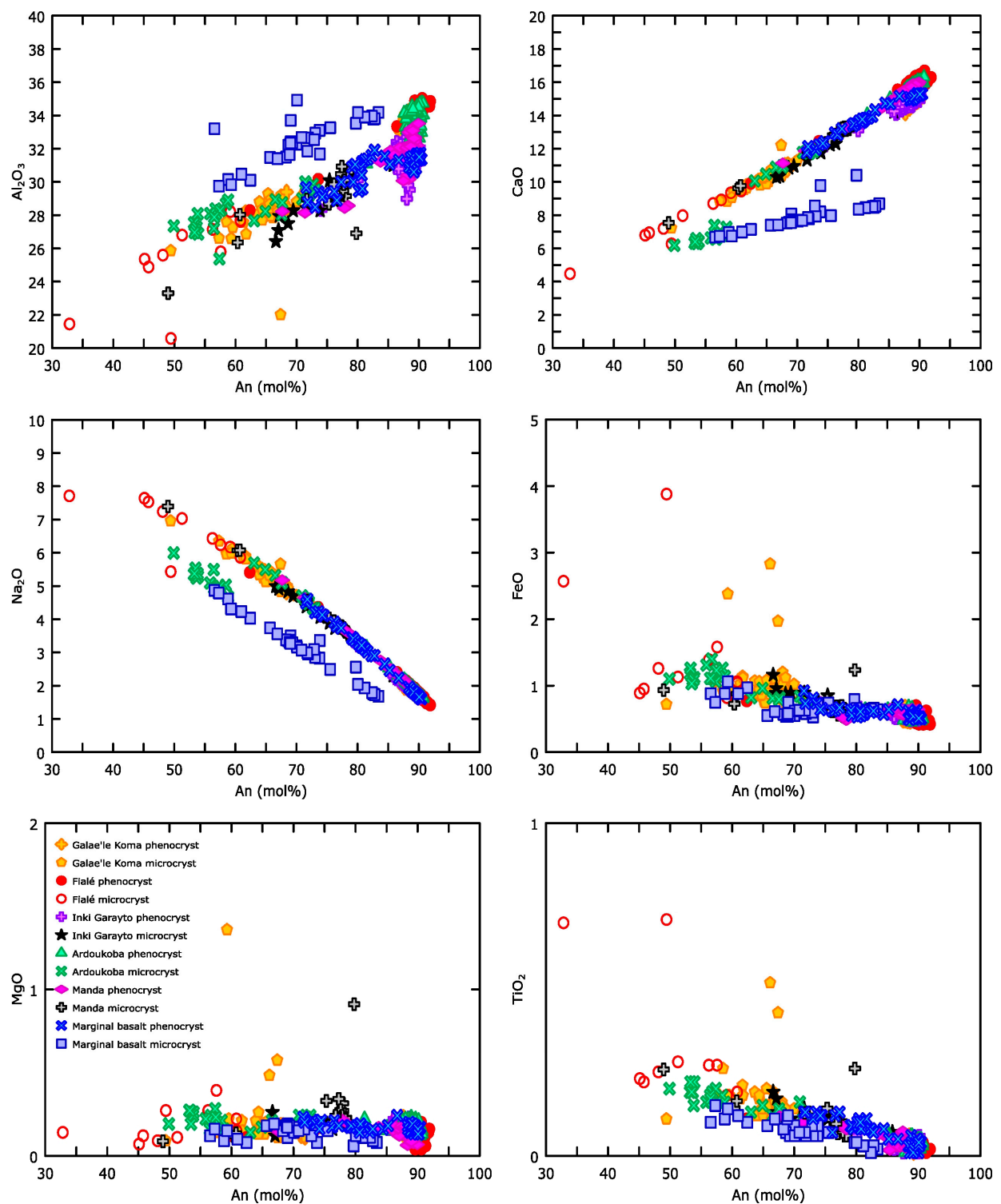


Figure 7. Major geochemical variation in Al₂O₃, CaO, Na₂O, FeO_T, and MgO versus An (mol%) for the Ardoukoba, Inki Garayto, Manda, Fialé, Galae'le Koma volcanoes and the marginal basalts.

Table 1. Melt H₂O calculated from the method described in [28] for the volcanoes located in the Asal–Ghoubbet area.

Volcano Name	Mineral	H ₂ O (wt.%) Max	H ₂ O (wt.%) Min	H ₂ O (wt.%) Average
Marginal basalts	Macrocryst	4.19	0.77	2.34
	Microcryst	1.60	0.23	1.08
Galaé’le Koma volcanoes	Macrocryst	3.90	2.58	3.38
	Microcryst	3.05	0.24	1.07
Fialé volcano	Macrocryst	4.42	2.37	3.46
	Microcryst	3.56	1.11	2.41
Manda volcano	Macrocryst	3.83	1.74	2.71
	Microcryst	3.22	2.00	2.80
Inki Garayto volcanoes	Macrocryst	4.15	2.39	3.20
	Microcryst	3.02	2.64	2.81
Ardoukoba volcano	Macrocryst	4.16	1.99	3.35
	Microcryst	2.65	0.58	1.71

5.3. Phase Equilibria

The equilibrium test between plagioclase and liquid was determined from anorthite (An) and albite (Ab) contents for macrocrysts and microcrysts to evaluate the equilibrium conditions for samples from all the volcanoes. Plagioclase macrocrysts of the marginal basalts have an average K_D of 0.57, and plagioclase microcrysts have an average K_D of 0.91. The plagioclase macrocrysts of Galaé’le Koma are in equilibrium (K_D 0.30 on average), but their microcrysts do not show equilibrium ($K_D = 0.79$). The macrocrysts of Fialé volcano, Manda volcano, Inki Garayto volcanoes, and Ardoukoba volcano have an average K_D of 0.33, 0.45, 0.46, and 0.31, respectively, and the average K_D of their microcrysts is 0.90, 1.15, 1.09, and 0.95. Accordingly, plagioclase microcrysts are generally not in equilibrium with the whole-rock compositions due to their relatively high content of Na₂O, which is more than 2 wt.%, and their anorthite contents, which are An < 60.

5.4. Plagioclase–Liquid Thermobarometry Calculations

A model was proposed by [28,29] to calculate the crystallization temperature and pressure of volcanic rocks, considering the equilibrium state between plagioclase and melt. In this model, to calculate the temperature and pressure of the plagioclase, the melt composition in equilibrium with the plagioclase must be known. An equilibrium test based on An–Ab exchange between plagioclase and melt was determined to demonstrate the equilibrium condition. According to this test, it can be said that plagioclase and melt are in equilibrium when $K_D(\text{An–Ab})_{\text{pl–melt}} = 0.10 \pm 0.5$, $T < 1050$ °C, and 0.27 ± 0.11 , $T > 1050$ °C. Temperature calculations were performed using the Putirka (2008) (24a) equation, and the [29] (25a) equation was used for pressure calculations. The temperature and pressure results of the investigated volcanic rocks are summarized in Table 2.

The macrocrysts and microcrysts in the marginal basalt present almost the same temperature and pressure values. The macrocrysts indicate a high temperature of 1216–1096 °C and a pressure of 14.51–9.05 kbar, while the microcrysts show corresponding values of 1203–1125 °C and 14.84–9.10 kbar (Table 2).

The thermobarometry results for the Galaé’le Koma volcanoes show that the macrocrysts exhibit temperatures of 1082–1174 °C with a pressure of 6.49–9.95 kbar (Table 2). The microcrysts occur in a temperature range of 1072 to 1186 °C and in a pressure range of 2.99 to 12.46 kbar. The microcrysts show a large gap in the pressure value, which may indicate a homogeneous-pressure eruption in the Galaé’le Koma volcanoes.

Table 2. Temperature [28] and pressure [29] values calculated for all volcanoes in the Asal–Ghoubbet area.

Volcano Name	Mineral	T (°C) Max	T (°C) Min	T (°C) Average	Pressure (P, kbar) Max	Pressure (P, kbar) Min	Pressure (P, kbar) Average
Marginal basalts	Macrocryst	1216	1096	1168	14.51	9.05	11.37
	Microcryst	1203	1125	1177	14.84	9.10	12.58
Galaé’le Koma volcanoes	Macrocryst	1174	1082	1131	9.95	6.49	8.10
	Microcryst	1186	1072	1156	12.46	2.99	5.51
Fialé volcano	Macrocryst	1161	1085	1124	12.58	3.92	8.24
	Microcryst	1159	1094	1126	10.09	4.00	6.26
Manda volcano	Macrocryst	1176	1107	1144	10.32	7.11	8.49
	Microcryst	1186	1098	1171	12.87	9.47	11.67
Inki Garayto volcanoes	Macrocryst	1172	1094	1133	13.67	6.72	9.11
	Microcryst	1186	1079	1146	12.70	8.23	11.18
Ardoukoba volcano	Macrocryst	1169	1085	1130	9.75	5.87	7.75
	Microcryst	1168	1100	1142	13.31	5.09	8.94

In Fialé volcano, the thermometry of the plagioclase macrocrysts presents a temperature of 1161 to 1085 °C, and the calculated pressure varies between 3.92 and 12.58 kbar. The microcrysts have a temperature range of 1159 to 1094 °C and a pressure of 4 to 10.09 kbar. In Fialé volcano, the calculated temperature of the macrocrysts and microcrysts is nearly the same, but there is a large gap in the pressure estimate.

In Manda volcano, the macrocryst temperature estimates range from 1107 to 1176 °C, and those of microcrysts range from 1198 to 1186 °C. The pressure estimates range from 7.11 to 10.32 kbar for the macrocrysts and 9.47 to 12.87 kbar for the microcrysts of Manda volcano.

The macrocrysts and microcrysts of the Inki Garayto volcanoes present similar temperatures and pressures. The thermobarometer using plagioclase provides a temperature of 1094–1172 °C for the macrocrysts and 1080–1186 °C for the microcrysts. Pressure estimates range from 6.72 to 13.67 kbar for the plagioclase macrocrysts and 8.23 to 12.70 kbar for the plagioclase microcrysts.

For Ardoukoba volcano, we calculated the temperature and pressure of pre-eruptive melt conditions from the plagioclase macrocrysts and microcrysts. The crystallization temperature of the plagioclase macrocrysts is 1082 to 1169 °C, while the temperature of the microcrysts is 1100 to 1168 °C. The calculated pressure ranges from 5.87 to 9.75 kbar for the macrocrysts and from 5.09 to 13.31 kbar for the microcrysts (Table 2).

5.5. Magma Reservoir Modeling

Our remarks on the plagioclase mineral chemistry of major elements and the thermobarometry of these minerals lead us to the existence of similarities in the magmatic system that formed the volcanic units in the Asal–Ghoubbet area. We suggest that a magma chamber might exist under the Asal–Ghoubbet feeding all the eruptions in the region.

To predict the emplacement depth for this magma chamber, we used the detailed chemical compositions of the plagioclases. This makes it easier to understand the depth of the magma source. The conversion factor of 1 kbar = 3.3 km provided by [30] was used to estimate the crystallization depth. In the marginal basalts, the crystallization depth was 29.87–47.88 km for the macrocrysts and 30.03–48.97 km for the microcrysts. The thermobarometry results of Galaé’le Koma volcanoes allow us to estimate that the crystallization depth of plagioclase macrocrysts is 21.42–32.84 km and the crystallization depth of microcrysts is 9.87–41.12 km. In Fialé volcano, the thermobarometry results of plagioclase indicate a crystallization depth corresponding to 12.94–41.51 km for the macrocrysts, and

the microcrysts have a depth ranging from 13.20 to 33.30 km. In Manda volcano, the crystallization depth corresponds to a depth of 23.46–34.06 km for the macrocrysts and 31.25–42.47 km for the microcrysts. In the Inki Garayto volcanoes, the estimated pressures of the macrocrysts and microcrysts reflect crystallization depths of 22.18–45.11 km and 27.16–41.91 km, respectively. The estimated depths of the macrocrysts and the microcrysts for the Ardoukoba volcano revealed crystallization depths of 19.37–32.18 km and 16.80–43.92 km, respectively. We summarize the depth calculations in Table 3 below.

Table 3. Depth calculation of different volcanic eruptions located in Asal–Ghoubbet area.

Volcano Name	Mineral	Pressure (P, kbar) Max	Pressure (P, kbar) Min	Depth (km)
Marginal basalts	Macrocryst	14.51	9.05	47.88–29.87
	Microcryst	14.84	9.10	48.97–30.03
Galaé’le Koma volcanoes	Macrocryst	9.95	6.49	32.84–21.42
	Microcryst	12.46	2.99	41.12–9.87
Fialé volcano	Macrocryst	12.58	3.92	41.51–12.94
	Microcryst	10.09	4.00	33.30–13.20
Manda volcano	Macrocryst	10.32	7.11	34.06–23.46
	Microcryst	12.87	9.47	42.47–31.25
Inki Garayto volcanoes	Macrocryst	13.67	6.72	45.11–22.18
	Microcryst	12.70	8.23	41.91–27.16
Ardoukoba volcano	Macrocryst	9.75	5.87	32.18–19.37
	Microcryst	13.31	5.09	43.92–16.80

The authors of [5] used a procedure for depth calculation based on [31,32] to determine the melting depth of magma. They found that melting paths beneath the inner floor range from 81 ± 4 to 43 ± 5 km and are consistent with adiabatic melting in the normal-temperature asthenosphere (1400 °C) beneath an extensively thinned mantle lithosphere. In the same procedure, the melting of the rift shoulder’s marginal basalts occurs beneath a thicker lithosphere, 107 ± 7 to 67 ± 8 km.

Normally, the crystallization of the plagioclase macrocrysts can take place in a deeper part than that of the microcrysts. However, the calculated thermodynamic value and the plagioclase depth formation are different for some volcanic formations, such as those in Galaé’le Koma, Manda, and Ardoukoba. We suggest the occurrence of early-stage microcryst crystallization in the magma chamber. Also, the plagioclase macrocrysts and microcrysts observed in the thin section and the rounded plagioclase noted in the hand specimen might be crystallized at the deeper part of the magma chamber and then act to rise up through a convection magma current.

Moreover, ref. [7] suggested a flotation phenomenon and proposed the interpretation for the Asal–Ghoubbet bytownites forming in a shallow-depth magma reservoir. Under these conditions, bytownites should separate by gravity, as should the ferromagnesian minerals olivine and pyroxene. Flotation phenomena may be responsible for the accumulation of bytownite megacrysts in the highest parts of the magma reservoir. Flotation, moreover, can explain the heterogeneity of the “crystal foam” and the fact that bytownites are associated with megacrysts of olivine and pyroxene which, being denser, should separate more easily by gravity [7]. If the magma is not too rich in gas and the pressure within the liquid is sufficient to allow the vesiculation of small bubbles, the latter will form at the solid–liquid interface and will act as floats. This process, which will lighten the crystals and promote their rise, will be facilitated by the fact that anorthite-rich plagioclases are very sensitive to absorption phenomena [33] in [7]. The presence of bubbles causes a reduction

in the apparent density of the magma, but this is not sufficient to prevent the slow rise of anorthite-rich plagioclase. The rare crystals that escape flotation are carried downward by the descending column of the convective cycle and can be partially resorbed. In the closed system of a magma chamber, the quantity and size of the bubbles increase upward, and it is difficult to imagine that this lightened magma can come back down. At the top of the magma chamber, an accumulation of “foam crystals” is formed, maintained at a high temperature by the thermal supply of the convective system [7].

On the basis of petrological data, it has been shown that the Asal–Ghoubbet volcanic formations were developed by fractional crystallization under low oxygen fugacity in a transitional basaltic magma [4]. The least fractionated are located in the rift margin series; the most evolved parts are found mainly in the series of the axial rift zone. These magmas extruded at Asal–Ghoubbet are therefore not of constant composition, but the variations observed over time are not random; they are linked to the chronological and structural evolution of the rift [4]. Some researchers believe that the source of the Asal–Ghoubbet magmas derived from two different sources corresponding to a stage in the evolution of the rift [4,34,35]: the magma from the axial zone whose tholeiitic character is the most marked and magma from the external and internal margins whose composition is intermediate [4]. Also, the magmas emplaced in the Asal–Ghoubbet volcanic formations do not constitute a unique series formed by fractionation from a single primary magma. Potentially, one magma was the origin of the basalts in the external margins and another magma formed the basalts in the internal margins and those of the axial series [34,35]. The different sizes of the plagioclase may explain the source and evolution of the magma reservoir of Asal–Ghoubbet-located volcanic eruptions. The PUB of Asal–Ghoubbet-located volcanic eruptions may explain the slow spreading of the rift by keeping the temperature for the crystallization of the macrocryst of the plagioclases at the magma chamber and then to their eruption after the magma supply from the mantle.

The plagioclase macrocrysts and microcrysts crystallized at various depths during the rising of magmas. In some volcanic formations, the rate of plagioclase phenocryst crystallization is rapid, so the grain size is very small; in other formations, the crystallization rate of macrocrysts is slow and the size is big. The crystal size increase is caused by the low decreasing ratio of the crystallization temperature, which increases the whole system. However, the rapid cooling of the magma forms small crystals in the system. The large crystal size of the macrocrysts resulted from magma that partially crystallized at depth and was transported upward to the chamber where the magma remained until it erupted. However, when observing the type of plagioclase and the chemical composition of macrocrysts and microcrysts, note that they are generally similar to each other. There is partial differentiation between different plagioclases from different volcanic eruptions, the different crystal sizes may rise because of the different crystallization depths during the eruptions. After each eruption, plagioclases always come out of the same source of the magma chamber, and the continuous crystallization at the bottom of the magma chamber feeds this crystallization process. There is a deep magma chamber, and these products come out of this magma chamber at various times.

All the volcanoes or volcanic formations in this area could be formed through fissure eruptions and volcanic cones. According to the thermobarometric calculation and estimated depth, it is revealed that all the volcanic units located in Asal–Ghoubbet might be crystallized mostly within the lithospheric mantle and have similar origins and almost similar crystallization depths. The thermobarometric and crystallization depth calculations show that the volcanic formations in the Asal–Ghoubbet area could be derived from multiple eruptions from a single magma chamber. Consequently, it is concluded that all the volcanic formations may be derived from a single magma chamber in convection which is located in the lowest part of the upper mantle. Therefore, we propose a magmatic model based on thermobarometry and the crystallization depth of plagioclases (Figure 8). We believe that such a model is essential to understanding the complexities of the Quaternary volcanic formations located in the Asal–Ghoubbet area. According to the geology, petrography, and

mineral chemistry of the plagioclases, all the volcanic eruptions located in Asal–Ghoubbet may be derived from the same magma chamber with different depths. However, the evolved Inki Garayto volcano derived from the magma chamber may have formed from an independent protrusion at the base level. This level may act to spread the source magma to form different anorthite contents during the crystallization of the Inki Garayto volcano in the Asal–Ghoubbet area.

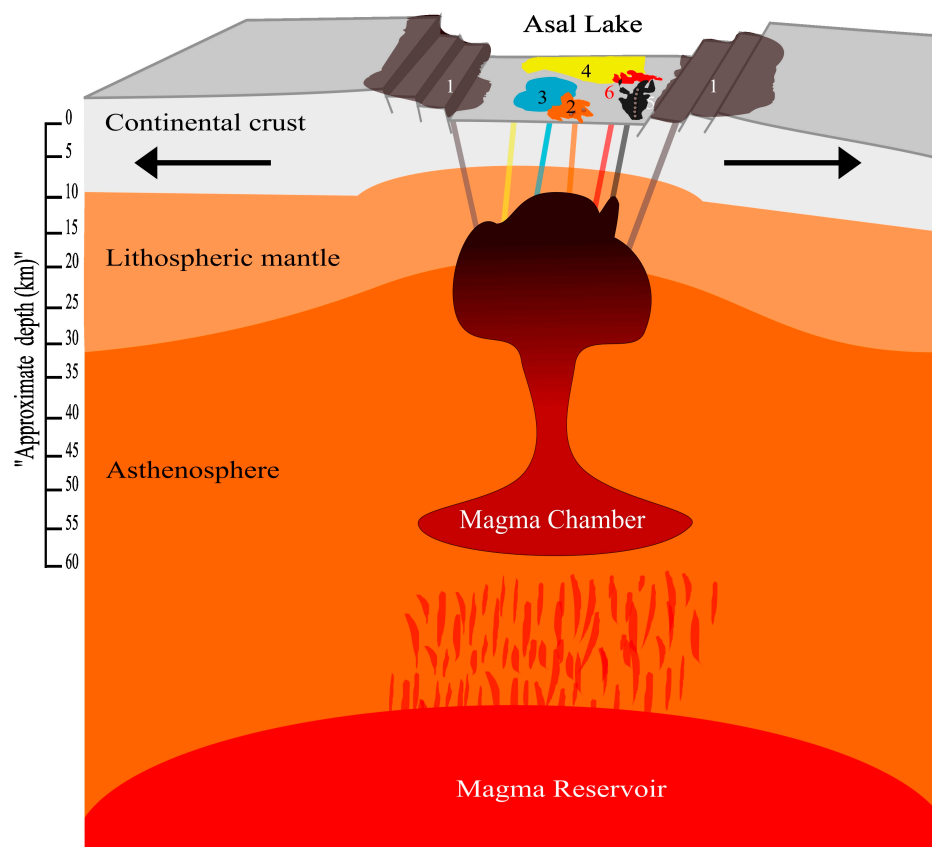


Figure 8. Conceptual model of magma plumbing system in Asal–Ghoubbet area. The lava flows of the marginal basalts, Galaé’le Koma, Fialé, Manda, Inki Garayto, and Ardoukoba are denoted by numbers 1 through 6, respectively.

6. Conclusions

This study aimed to provide information about the magma source of the volcanic formations in the Asal–Ghoubbet Rift. Confocal Raman spectroscopy and mineral chemistry revealed that the rounded and unusually large (up to 4 cm) plagioclase macrocrysts are bytownite, and the microcrysts are labradorite to andesine. The plagioclase macrocrysts have reached the rounded shape by circling within the magma chamber due to a convection current at the central part of the magma chamber. The plagioclase ultraphyric basalt of the Asal–Ghoubbet area may indicate the slow spreading and the keeping of the high temperature for the growth of the macrocrysts of the plagioclases within the magma chamber. The model-derived plagioclase macrocryst and microcryst crystallization temperature and pressure for these volcanic formations are 1072 to 1216 °C and 2.99 to 14.84 kbar, respectively, and the calculated H₂O contents of the formation magmas range from 0.23 to 4.42 wt.%.

The obtained thermobarometric values suggest that the magma source of the marginal basalt is located at a depth of 34–55 km, the Galaé’le Koma volcanoes were fed by a magma reservoir at about 11–46 km depth, Fialé volcano was tapped directly from a depth of 15–47 km, the eruption of Manda volcano was sourced from a magma stored at 26–48 km

depth, Inki Garayto was sourced from a depth of 25–51 km, and Ardoukoba volcano was sourced from a magma reservoir at about 19–49 km depth.

The geochemical signatures of the plagioclases exhibit similar characteristics, which indicates that these plagioclases came from a magma source that may be related. Although the crystallization depths differ among the plagioclases from the various volcanic formations, based on the correlation of the geochemical composition of megacrysts of macrocrysts and microcrysts, it appears that these separate volcanic formations were derived from the same magma located beneath Asal–Ghoubbet.

Supplementary Materials: The following supporting information can be downloaded at <https://www.mdpi.com/article/10.3390/min14030216/s1>: Figure S1: Raman spectra of plagioclases from the marginal basalts, Manda volcano, and Ardoukoba volcano; Figure S2: Raman spectra of plagioclases from the Galaé'le Koma volcanoes, Fialé volcano, and Inki Garayto volcanoes; Table S1: Whole-rock major element geochemistry of all volcanic formations located in the Asal–Ghoubbet area; Table S2: Plagioclase mineral chemistry results for Ardoukoba volcano; Table S3: Plagioclase mineral chemistry results for Fialé volcano; Table S4: Plagioclase mineral chemistry results for the Galaé'le Koma volcanoes; Table S5: Plagioclase mineral chemistry results for the Inki Garayto volcanoes; Table S6: Plagioclase mineral chemistry results for Manda volcano; Table S7: Plagioclase mineral chemistry results for the marginal basalt.

Author Contributions: A.D.I.: fieldwork, conceptualization, methodology, investigation, writing, review, and editing. Y.K.K.: visualization, supervision, formal analysis, contributed to interpretive aspects, editing, and reviewed the original draft manuscript. All authors have read and agreed to the published version of the manuscript.

Funding: This research received no external funding.

Data Availability Statement: Data are contained within the article.

Acknowledgments: We thank Kıymet Deniz YAĞCIOĞLU for her valuable support and help with the EPMA and confocal Raman spectroscopy analytical work. We warmly thank Abdourahman O. Haga, Moussa Hassanleh, and Araksan Aden for their precious support during sample collections and field study. We would also like to acknowledge Kayad Moussa for logistical support and accommodation during the field trip in the Asal–Ghoubbet area.

Conflicts of Interest: The authors declare no conflicts of interest.

References

1. Stieltjes, L. L'axe Tectono-Volcanique d'Asal (Afar Central—T.F.A.I.). Ph.D. Thesis, Paris-Sud University, Paris, France, 1973.
2. Vellutini, P. The Manda—Inakir rift, republic of Djibouti: A comparison with the Asal rift and its geodynamic interpretation. *Tectonophysics* **1990**, *172*, 141–153. [\[CrossRef\]](#)
3. Vellutini, P.; Piguet, P.; Recroix, F.; Demange, J.; Abdallah, A. Carte Géologique de la République de Djibouti au 1/100000: Notice d'Asal. Edition BRGM. Published online 1993. Available online: https://drive.google.com/file/d/12CfK-0RyH_-JAI5Fhcb7HWEB75-E_j-C/view (accessed on 22 January 2024).
4. Stieltjes, L.; Joron, J.L.; Treuil, M.; Varet, J. Le rift d'Asal, segment de dorsale emerge; discussion petrologique et geochemique. *Bull. Société Géologique Fr. Bull. Soc. Geol. Fr.* **1976**, *18*, 851–862. [\[CrossRef\]](#)
5. Pinzuti, P.; Humler, E.; Manighetti, I.; Gaudemer, Y. Petrological constraints on melt generation beneath the Asal Rift (Djibouti) using quaternary basalts. *Geochem. Geophys. Geosyst.* **2013**, *14*, 2932–2953. [\[CrossRef\]](#)
6. Iltireh, A.D. Petrology of Volcanic Rocks from Asal-Ghoubet Area: Magma Genesis and Its Evolution, Djibouti. Ph.D. Dissertation, Ankara University, Ankara, Turkey, 2024.
7. Bizouard, H.; Clocchiatti, R.; Marinelli, G. Les tholeiites a olivine a megacristsaux de bytownite du rift d'Asal (Republique de Djibouti); quelques suggestions pour un modele genetique. *Bull. Soc. Geol. Fr.* **1980**, *22*, 845–850. [\[CrossRef\]](#)
8. Flower, M.F.J. Accumulation of calcic plagioclase in ocean-ridge tholeiite: An indication of spreading rate? *Nature* **1980**, *287*, 530–532. [\[CrossRef\]](#)
9. Hansen, H.; Grönvold, K. Plagioclase ultraphyric basalts in Iceland: The mush of the rift. *J. Volcanol. Geotherm. Res.* **2000**, *98*, 1–32. [\[CrossRef\]](#)
10. Lange, A.E.; Nielsen, R.L.; Tepley, I.I.F.J.; Kent, A.J.R. The petrogenesis of plagioclase-phyric basalts at mid-ocean ridges. *Geochem. Geophys. Geosyst.* **2013**, *14*, 3282–3296. [\[CrossRef\]](#)
11. Ruegg, J.C.; Kasser, M. Deformation across the Asal-Ghoubbet Rift, Djibouti, Uplift and crustal extension 1979–1986. *Geophys. Res. Lett.* **1987**, *14*, 745–748. [\[CrossRef\]](#)

12. Manighetti, I.; Tapponnier, P.; Gillot, P.Y.; Jacques, E.; Courtillot, V.; Armijo, R.; Ruegg, J.C.; King, G. Propagation of rifting along the Arabia-Somalia Plate Boundary: Into Afar. *J. Geophys. Res. Solid Earth* **1998**, *103*, 4947–4974. [\[CrossRef\]](#)
13. Jacques, E.; King, G.C.P.; Tapponnier, P.; Ruegg, J.C.; Manighetti, I. Seismic activity triggered by stress changes after the 1978 events in the Asal Rift, Djibouti. *Geophys. Res. Lett.* **1996**, *23*, 2481–2484. [\[CrossRef\]](#)
14. Tazieff, H.; Varet, J.; Barberi, F.; Giglia, G. Tectonic Significance of the Afar (or Danakil) Depression. *Nature* **1972**, *235*, 144–147. [\[CrossRef\]](#)
15. Needham, H.D.; Choukroune, P.; Cheminee, J.L.; Le Pichon, X.; Francheteau, J.; Tapponnier, P. The accreting plate boundary Ardoukôba Rift (northeast Africa) and the oceanic Rift Valley. *Earth Planet. Sci. Lett.* **1976**, *28*, 439–453. [\[CrossRef\]](#)
16. Harrison, C.G.A.; Bonatti, E.; Stieltjes, L. Tectonism of Axial Valleys in Spreading Centers: Data from the Afar Rift, Afar Depression of Ethiopia, 1 A. Pilger, A. Rösler, 178–198. Published online 1975.
17. Courtillot, V.; Achache, J.; Landre, F.; Bonhommet, N.; Montigny, R.; Féraud, G. Episodic spreading and rift propagation: New paleomagnetic and geochronologic data from the Afar nascent passive margin. *J. Geophys. Res. Solid Earth* **1984**, *89*, 3315–3333. [\[CrossRef\]](#)
18. Stieltjes, L. *Geological Map of Asal Rift. Republic of Djibouti, Scale 1/50000*; Bureau de Recherches Géologiques et Minières: Orléans, France, 1980.
19. Vidal, P.; Deniel, C.; Vellutini, P.J.; Piguet, P.; Coulon, C.; Vincent, J.; Audin, J. Changes of mantle sources in the course of a rift evolution: The Afar case. *Geophys. Res. Lett.* **1991**, *18*, 1913–1916. [\[CrossRef\]](#)
20. Deniel, C.; Vidal, P.; Coulon, C.; Vellutini, P.; Piguet, P. Temporal evolution of mantle sources during continental rifting: The volcanism of Djibouti (Afar). *J. Geophys. Res. Solid Earth* **1994**, *99*, 2853–2869. [\[CrossRef\]](#)
21. Koralay, T.; Kadioglu, Y.K. Reasons of different colors in the ignimbrite lithology: Micro-XRF and confocal Raman spectrometry method. *Spectrochim. Acta A Mol. Biomol. Spectrosc.* **2008**, *69*, 947–955. [\[CrossRef\]](#) [\[PubMed\]](#)
22. Koralay, T. Petrographic and geochemical characteristics of upper Miocene Tekkedag volcanics (Central Anatolia—Turkey). *Geochemistry* **2010**, *70*, 335–351. [\[CrossRef\]](#)
23. Kadioglu, Y.K.; Üstündağ, Z.; Deniz, K.; Yenikaya, C.; Erdoğan, Y. XRF and Raman Characterization of Antimonite. *Instrum. Sci. Technol.* **2009**, *37*, 683–696. [\[CrossRef\]](#)
24. Deniz, K. Mica Types as Indication of Magma Nature, Central Anatolia, Turkey. *Acta Geol. Sin. -Engl. Ed.* **2022**, *96*, 844–857. [\[CrossRef\]](#)
25. İltireh, A.D.; Kadioglu, Y.K. Geochemistry and Petrogenesis of Inki-Garayto Volcano in Asal-Ghoubbet area, Republic of Djibouti. In Proceedings of the 8th International Black Sea Coastline Countries Scientific Research Conference, Sofia, Bulgaria, 29–30 August 2022; pp. 884–893.
26. Hattori, K.; Sato, H. Magma evolution recorded in plagioclase zoning in 1991 Pinatubo eruption products. *Am. Mineral.* **1996**, *81*, 982–994. [\[CrossRef\]](#)
27. Joron, J.L.; Treuil, M.; Jaffrezic, H.; Villemant, B. Etude geochemique des elements en traces dans les series de roches volcaniques du rift d’Asal; identification et analyse des processus d’accrétion. *Bull. Soc. Geol. Fr.* **1980**, *7*, 851–861. [\[CrossRef\]](#)
28. Putirka, K.D. Thermometers and Barometers for Volcanic Systems. *Rev. Miner. Geochem.* **2008**, *69*, 61–120. [\[CrossRef\]](#)
29. Putirka, K.D. Igneous thermometers and barometers based on plagioclase + liquid equilibria: Tests of some existing models and new calibrations. *Am. Mineral.* **2005**, *90*, 336–346. [\[CrossRef\]](#)
30. Putirka, K.; Johnson, M.; Kinzler, R.; Longhi, J.; Walker, D. Thermobarometry of mafic igneous rocks based on clinopyroxene-liquid equilibria, 0–30 kbar. *Contrib. Mineral. Petrol.* **1996**, *123*, 92–108. [\[CrossRef\]](#)
31. Klein, E.M.; Langmuir, C.H. Global correlations of ocean ridge basalt chemistry with axial depth and crustal thickness. *J. Geophys. Res. Solid Earth* **1987**, *92*, 8089–8115. [\[CrossRef\]](#)
32. Langmuir, C.H.; Klein, E.M.; Plank, T. Petrological systematics of mid-ocean ridge basalts: Constraints on melt generation beneath ocean ridges. In *Mantle Flow and Melt Generation at Mid-Ocean Ridges*; American Geophysical Union: Washington, DC, USA, 1992; pp. 183–280.
33. Gaudin, A.M. *Flottation*. Ed; McGraw-Hill: New York, NY, USA, 1932.
34. Treuil, M.; Varet, J. Criteres volcanologiques, petrologiques et geochimiques de la genese et de la differenciation des magmas basaltiques; exemple de l’Afar. *Bull. Soc. Geol. Fr.* **1973**, *7*, 506–540. [\[CrossRef\]](#)
35. Treuil, M.; Joron, J.L. Utilisation des propriétés des éléments fortement hygromagmatophiles pour l’étude de la composition chimique et de l’hétérogénéité du manteau. *Bull. Soc. Geol. Fr.* **1977**, *19*, 1197–1205.

Disclaimer/Publisher’s Note: The statements, opinions and data contained in all publications are solely those of the individual author(s) and contributor(s) and not of MDPI and/or the editor(s). MDPI and/or the editor(s) disclaim responsibility for any injury to people or property resulting from any ideas, methods, instructions or products referred to in the content.